

UPDATE ON MINIMAL SUPERSYMMETRIC HYBRID INFLATION IN LIGHT OF PLANCK

CONSTANTINOS PALLIS¹ AND QAISAR SHAFI²

¹*Department of Physics, University of Cyprus, P.O. Box 20537, Nicosia 1678, CYPRUS*
e-mail address: cpallis@ucy.ac.cy

²*Bartol Research Institute, Department of Physics and Astronomy, University of Delaware, Newark, DE 19716, USA*
e-mail address: shafi@bartol.udel.edu

ABSTRACT: The minimal supersymmetric (or F-term) hybrid inflation is defined by a unique renormalizable superpotential, fixed by a $U(1)$ R-symmetry, and it employs a canonical Kähler potential. The inflationary potential takes into account both radiative and supergravity corrections, as well as an important soft supersymmetry breaking term, with a mass coefficient in the range $(0.1 - 10)$ TeV. The latter term assists in obtaining a scalar spectral index n_s close to 0.96, as strongly suggested by the PLANCK and WMAP-9yr measurements. The minimal model predicts that the tensor-to-scalar r is extremely tiny, of order 10^{-12} , while the spectral index running, $|dn_s/d \ln k| \sim 10^{-4}$. If inflation is associated with the breaking of a local $U(1)_{B-L}$ symmetry, the corresponding symmetry breaking scale M is $(0.7 - 1.6) \cdot 10^{15}$ GeV with $n_s \simeq 0.96$. This scenario is compatible with the bounds on M from cosmic strings, formed at the end of inflation from $B - L$ symmetry breaking. We briefly discuss non-thermal leptogenesis which is readily implemented in this class of models.

PACs numbers: 98.80.Cq, 12.60.Jv

Published in Phys. Lett. B **725**, 327 (2013)

I. INTRODUCTION

Supersymmetric (SUSY) hybrid inflation based on F-terms, also referred to as *F-term hybrid inflation* (FHI), is one of the simplest and well-motivated inflationary models [1, 2]. It is tied to a renormalizable superpotential uniquely determined by a global $U(1)$ R-symmetry, does not require fine tuned parameters, and it is naturally associated with the breaking of a local symmetry, such as $G_{B-L} = G_{\text{MSSM}} \times U(1)_{B-L}$ [3], where $G_{\text{MSSM}} = SU(3)_C \times SU(2)_L \times U(1)_Y$ is the gauge group of the *Minimal Supersymmetric Standard Model* (MSSM) or, $G_{\text{LR}} = SU(2)_L \times SU(2)_R \times U(1)_{B-L}$ [4], flipped $SU(5)$ [5], etc. As shown in Ref. [1], the addition of *radiative corrections* (RCs) to the tree level inflationary potential predicts a scalar spectral index $n_s \simeq 0.98$, and the microwave temperature anisotropy $\Delta T/T$ is proportional to $(M/m_{\text{P}})^2$, where M denotes the scale of the gauge symmetry breaking. It turns out that M usually is not far from $M_{\text{GUT}} \simeq (2 - 3) \cdot 10^{16}$ GeV. Here $m_{\text{P}} = 2.4 \cdot 10^{18}$ GeV is the reduced Planck mass. A more complete treatment [6], which incorporates *supergravity* (SUGRA) corrections [7] with canonical (minimal) Kähler potential, as well as an important soft SUSY breaking term [8], can yield lower n_s values (0.95 – 0.97). Recall that the minimal Kähler potential insures that the SUGRA corrections do not spoil the flatness of the potential that is required to implement FHI – reduction of n_s by invoking non-minimal Kähler potentials is analyzed in Ref. [9–11].

Insisting on the simplest realization of FHI – and the one-step inflationary paradigm, cf. Ref. [12] – we wish to emphasize here that FHI is in good agreement, in a rather narrow but well-defined range of its parameters, with the latest WMAP [13] and PLANCK [14] data pertaining to the Λ CDM framework. To this end, SUGRA [7] and soft SUSY breaking [6, 8] corrections are taken into account, in addition to the well-known [1] RCs. The minimality of the model is justified by the fact that FHI is implemented within *minimal supergravity* (mSUGRA) and within a minimal extension of G_{MSSM} , obtained by promoting the pre-existing global $U(1)_{B-L}$ sym-

metry of MSSM to a local one. As a consequence, three *right-handed neutrinos*, ν_i^c , are necessary to cancel the anomalies. The presence of ν_i^c leads to a natural explanation for the observed [15] *baryon asymmetry of the universe* (BAU) via *non-thermal leptogenesis* (nTL) [16], and the existence of tiny but non-zero neutrino masses. As we show, this set-up is compatible with the gravitino constraint [17, 18] and the current data [19, 20] on the neutrino oscillation parameters. It is worth mentioning that our scenario fits well with the bound [21] induced by the non-observation of the cosmic strings, formed during the $B - L$ phase transition. Note that strings may serve as a source [22] of a controllable amount of non-gaussianity in the cosmic microwave background anisotropy.

In the following discussion, we briefly review the minimal FHI and present our updated results in Sec. II. We then consider nTL using updated constraints from neutrino physics in Sec. III. Our conclusions are summarized in Sec. IV.

II. MINIMAL FHI MODEL

A. GENERAL SET-UP. The minimal FHI is based on the superpotential

$$W_{\text{HI}} = \kappa S (\bar{\Phi}\Phi - M^2), \quad (1)$$

where $\bar{\Phi}$, Φ denote a pair of chiral superfields oppositely charged under $U(1)_{B-L}$, S is a G_{B-L} -singlet chiral superfield, and the parameters κ and M are made positive by field redefinitions. W_{HI} is the most general renormalizable superpotential consistent with a continuous R-symmetry [1] under which $S \rightarrow e^{i\alpha} S$, $\bar{\Phi}\Phi \rightarrow \bar{\Phi}\Phi$, $W \rightarrow e^{i\alpha} W$. The SUSY potential, V_{SUSY} , extracted (see e.g. Ref. [23, 24]) from W_{HI} in Eq. (1) includes F and D-term contributions. Along the direction $|\bar{\Phi}| = |\Phi|$, the latter contribution vanishes whereas the former reads

$$V_{\text{SUSY}} = \kappa^2 ((|\Phi|^2 - M^2)^2 + 2|S|^2|\Phi|^2). \quad (2)$$

The scalar components of the superfields are denoted by the same symbols as the corresponding superfields. Restricting

ourselves to the D-flat direction, from V_{SUSY} in Eq. (2) we find that the SUSY vacuum lies at

$$\langle S \rangle = 0 \quad \text{and} \quad |\langle \Phi \rangle| = |\langle \bar{\Phi} \rangle| = M. \quad (3)$$

As a consequence, W_{HI} leads to the spontaneous breaking of G_{B-L} , to G_{MSSM} with SUSY unbroken.

The superpotential W_{HI} also gives rise to FHI since, for values of $|S| \gg M$, there exist a flat direction

$$\bar{\Phi} = \Phi = 0 \quad \text{with,} \quad V_{\text{SUSY}} (\bar{\Phi} = \Phi = 0) \equiv V_{\text{HI0}} = \kappa^2 M^4. \quad (4)$$

Thus, V_{HI0} provides us with a constant potential energy density which can be used to implement FHI.

B. THE INFLATIONARY POTENTIAL. The inflationary potential of minimal FHI, to a good approximation, can be written as

$$V_{\text{HI}} = V_{\text{HI0}} + V_{\text{HIC}} + V_{\text{HIS}} + V_{\text{HIT}}, \quad (5)$$

where, besides the dominant contribution V_{HI0} in Eq. (4), V_{HI} includes the following contributions:

- V_{HIC} represents the RCs to V_{HI} originating from a mass splitting in the $\Phi - \bar{\Phi}$ supermultiplets, caused by SUSY breaking along the inflationary valley [1]:

$$V_{\text{HIC}} = \frac{\kappa^2 N}{32\pi^2} V_{\text{HI0}} \left(2 \ln \frac{\kappa^2 x M^2}{Q^2} + f_{\text{rc}}(x) \right), \quad (6a)$$

where $N = 1$ is the dimensionality of the representations to which $\bar{\Phi}$ and Φ belong, Q is a renormalization scale, $x = \sigma^2/2M^2$ with $\sigma = \sqrt{2}|S|$ being the canonically normalized inflaton field, and

$$f_{\text{rc}}(x) = (x+1)^2 \ln(1+1/x) + (x-1)^2 \ln(1-1/x). \quad (6b)$$

- V_{HIS} is the SUGRA correction to V_{HI} [7, 8]:

$$V_{\text{HIS}} = V_{\text{HI0}} \sigma^4 / 8m_{\text{P}}^4, \quad (7)$$

where we employ the canonical Kähler potential $K = |S|^2 + |\Phi|^2 + |\bar{\Phi}|^2$ working within mSUGRA.

- V_{HIT} is the most important contribution to V_{HI} from the soft SUSY effects [6, 8] parameterized as follows:

$$V_{\text{HIT}} = -a_S \sigma \sqrt{V_{\text{HI0}}/2}, \quad (8)$$

where [4, 6] $a_S = 2|2 - A|m_{3/2} \cos(\theta_S + \theta_{(2-A)})$ is the tadpole parameter which takes values comparable to $m_{3/2} \sim (0.1 - 10)$ TeV, the gravitino, \tilde{G} , mass. The soft SUSY breaking mass² term for S , with mass $\sim m_{3/2}$, is negligible [10] for FHI. Also, A is the dimensionless trilinear coupling, of order unity, associated with the first term of W_{HI} in Eq. (1). Imposing the condition $\theta_S + \theta_{(2-A)} = 0 \pmod{2\pi}$, V_{HI} is minimized *with respect to* (w.r.t.) the phases θ_S and $\theta_{(2-A)}$ of S and $(2 - A)$ respectively. We further assume that θ_S remains constant during FHI.

C. THE INFLATIONARY OBSERVABLES – REQUIREMENTS. Under the assumptions that (i) the curvature perturbation generated by σ is solely responsible for the one that is observed, and (ii) FHI is followed in turn by a decaying-particle, radiation and matter domination, the parameters of our model can be restricted by requiring that:

- The number of e-foldings $N_{\text{HI}*}$ that the scale $k_* = 0.05/\text{Mpc}$ undergoes during FHI leads to a solution of the horizon and flatness problems of standard big bang cosmology. Employing standard methods [11, 14, 24], we can derive the relevant condition:

$$N_{\text{HI}*} \equiv \int_{\sigma_f}^{\sigma_*} \frac{d\sigma}{m_{\text{P}}^2} \frac{V_{\text{HI}}}{V'_{\text{HI}}} \simeq 19.4 + \frac{2}{3} \ln \frac{V_{\text{HI0}}^{1/4}}{1 \text{ GeV}} + \frac{1}{3} \ln \frac{T_{\text{rh}}}{1 \text{ GeV}}, \quad (9)$$

where T_{rh} is the reheat temperature after FHI, the prime denotes derivation w.r.t. σ , σ_* is the value of σ when k_* crossed outside the horizon of FHI, and σ_f is the value of σ at the end of FHI. This coincides with either the critical point $\sigma_c = \sqrt{2}M$ appearing in the particle spectrum of $\Phi - \bar{\Phi}$ system during FHI – see Eq. (6b) – or the value for which one of the slow-roll parameters [24]

$$\epsilon \simeq m_{\text{P}}^2 (V'_{\text{HI}}/V_{\text{HI}})^2 / 2 \quad \text{and} \quad \eta \simeq m_{\text{P}}^2 V''_{\text{HI}}/V_{\text{HI}} \quad (10)$$

exceeds unity. In our scheme, we exclusively find $\sigma_f = \sigma_c$. Since the resulting κ values are sizably larger than $(M/m_{\text{P}})^2$ – see next section – we do not expect the production of extra e-foldings during the waterfall regime, which in our case turns out to be nearly instantaneous – cf. Ref. [25].

- The amplitude, A_s , of the power spectrum of the curvature perturbation, which is generated during FHI and calculated at k_* as a function of σ_* , is consistent with the data [13, 14], i.e.

$$A_s^{1/2} = \frac{1}{2\sqrt{3}\pi m_{\text{P}}^3} \frac{V_{\text{HI}}^{3/2}(\sigma_*)}{|V'_{\text{HI}}(\sigma_*)|} \simeq 4.685 \cdot 10^{-5}. \quad (11)$$

- The (scalar) spectral index n_s , its running, $dn_s/d \ln k \equiv \alpha_s$, and the scalar-to-tensor ratio, r , which are given by

$$n_s = 1 - 6\epsilon_* + 2\eta_*, \quad (12a)$$

$$\alpha_s = 2(4\eta_*^2 - (n_s - 1)^2) / 3 - 2\xi_* \quad \text{and} \quad r = 16\epsilon_*, \quad (12b)$$

where $\xi \simeq m_{\text{P}}^4 V'_{\text{HI}} V'''_{\text{HI}} / V_{\text{HI}}^2$ and all variables with the subscript $*$ are evaluated at $\sigma = \sigma_*$, should be in agreement with the following values [13, 14] based on the Λ CDM model:

$$n_s = 0.9603 \pm 0.014 \Rightarrow 0.946 \lesssim n_s \lesssim 0.975, \quad (13a)$$

$$\alpha_s = -0.0134 \pm 0.018, \quad \text{and} \quad r < 0.11, \quad (13b)$$

at 95% *confidence level* (c.l.).

- The tension μ_{cs} of the $B - L$ cosmic strings produced at the end of FHI respects the bound [21] – cf. Ref. [26–28]:

$$\mu_{\text{cs}} \approx 9.6\pi M^2 / \ln(2/\beta) \lesssim 8 \cdot 10^{-6} m_{\text{P}}^2. \quad (14)$$

Here, we adapt to our set-up the results of the simulations for the abelian Higgs model following Ref. [29], $\beta = \kappa^2/8g^2 \leq 10^{-2}$, with $g \simeq 0.7$ being the gauge coupling constant close to M_{GUT} . Note that the presence of strings does not anymore [30] allow n_s closer to unity.

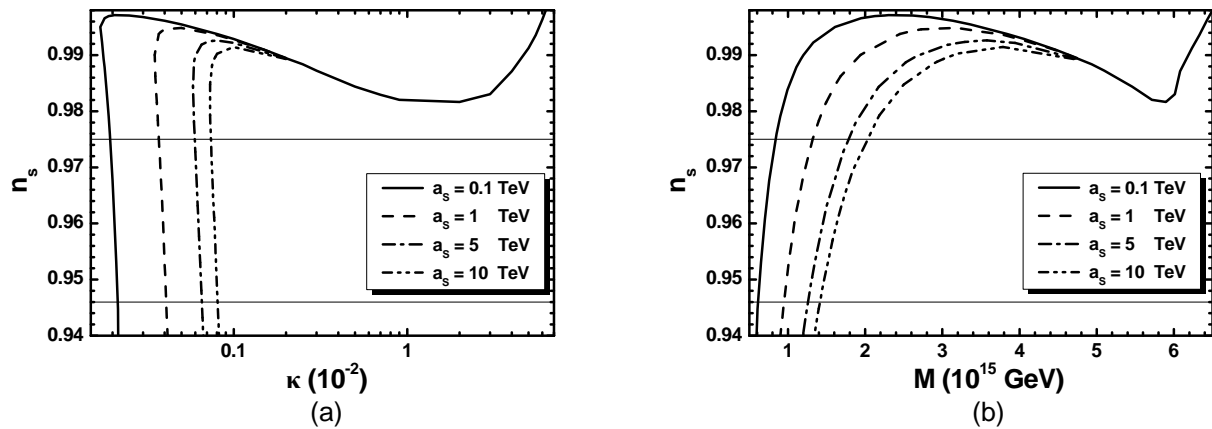


FIG. 1: n_s versus κ (a), and n_s versus M (b) for $a_S = 0.1$ TeV (solid lines), $a_S = 1$ TeV (dashed lines), $a_S = 5$ TeV (dot-dashed lines) and $a_S = 10$ TeV (double dot-dashed lines). The two horizontal lines are based on Eq. (13a)

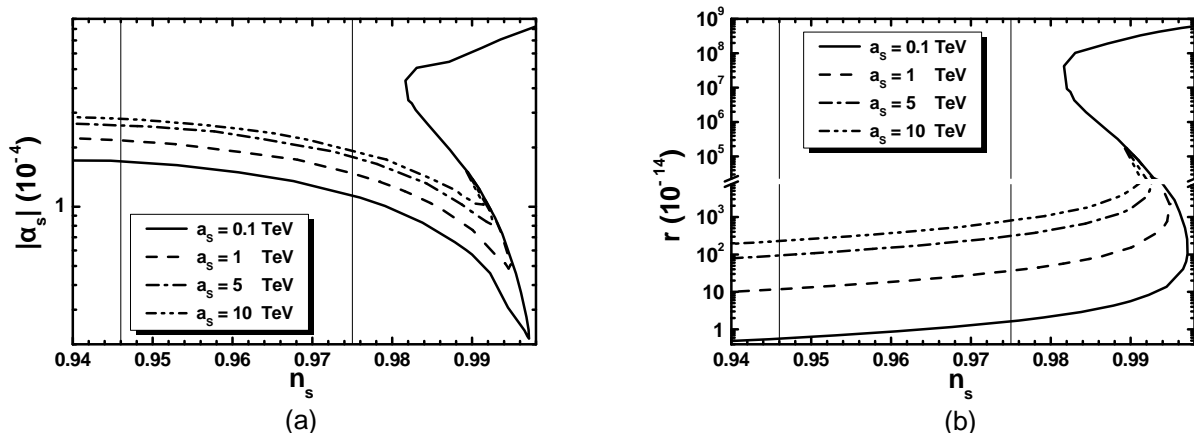


FIG. 2: $|\alpha_s|$ versus n_s (a), and r versus n_s (b) respectively. Vertical lines arise from Eq. (13a).

D. RESULTS. The investigation of our model depends on the parameters:

$$\kappa, M, a_S, T_{\text{rh}}, \text{ and } \sigma_*.$$

In our computation, we use as input parameters a_S and κ , and fix $T_{\text{rh}} \simeq 5 \cdot 10^8$ GeV, as suggested by our results in Sec. III. Variation of T_{rh} over 1–2 orders of magnitude is not expected to significantly alter our findings – see Eq. (9). We then restrict M and σ_* so that Eqs. (9) and (11) are fulfilled. Using Eqs. (12a) and (12b), we can extract the values for n_s , α_s and r , thereby testing our model against the observational data of Eqs. (13a) and (13b).

Our results are presented in Figs. 1, 2 and 3 taking $a_S = 0.1$ TeV (solid lines), $a_S = 1$ TeV (dashed lines), $a_S = 5$ TeV (dot-dashed lines), and $a_S = 10$ TeV (double dot-dashed lines). In Figs. 1 and 2 the observationally compatible region of Eq. (13a) is also indicated by the horizontal (in Fig. 1) or vertical (in Fig. 2) lines. For the sake of clarity, we do not show solutions with $M > 2 \cdot 10^{16}$ GeV – cf. Ref. [6] – which are totally excluded by Eq. (13a).

From Fig. 1, where we depict n_s versus κ (a) and M (b),

we note that, for $\kappa \gtrsim 0.002$ and $M \gtrsim 4.7 \cdot 10^{15}$ GeV, V_{HIC} and progressively – for $\kappa \gtrsim 0.04$ and $M \gtrsim 6.1 \cdot 10^{15}$ GeV, – V_{HIS} dominates V_{HI} in Eq. (5), and drives n_s to values close to or larger than 0.98, independently of the selected a_S values. On the other hand, for $\kappa \lesssim 0.002$, V_{HIT} starts becoming comparable to V_{HIC} and succeeds in reconciling n_s with Eq. (13a) for well defined κ (and M) values that are related to the chosen a_S . Actually, for the allowed n_s , we find that $V_{\text{HIC}}/V_{\text{HIT}} \simeq 13$, whereas V_{HIS} turns out to be totally negligible. Fixing n_s to its central value in Eq. (13a), we display in Table I the values for (κ, M) corresponding to the a_S values employed in Figs. 1-3.

From our numerical computations we observe that, in the regime with acceptable n_s values, the σ_* required by Eqs. (9) and (11) becomes comparable to σ_c , and $f_{\text{rc}}(x)$ in Eq. (6b) can be approximated as [11]

$$f_{\text{rc}}(x) \simeq 3 - \frac{x^{-2}}{6} - \frac{x^{-4}}{30} - \frac{x^{-6}}{84} - \frac{x^{-8}}{180} - \frac{x^{-10}}{330} - \frac{x^{-12}}{546} - \frac{x^{-14}}{840} - \frac{x^{-16}}{1224} - \frac{x^{-18}}{1710} - \frac{x^{-20}}{2310}. \quad (15)$$

TABLE I: Model parameters and predictions for $n_s \simeq 0.96$.

a_S (TeV)	κ (10^{-4})	M (10^{15} GeV)	Δ_{c^*} (%)	Δ_{\max^*} (%)	$-\alpha_s$ (10^{-4})	r (10^{-13})
0.1	2.05	0.7	0.6	0.016	1.5	0.09
1	3.9	1.1	2	1.2	1.9	1.9
5	6.3	1.4	4.3	2.8	2.4	15
10	7.7	1.6	6.3	3.8	2.5	38

Moreover, in the vicinity of σ_* , V_{HI} develops a local maximum at σ_{\max} allowing for FHI of hilltop type [31] to take place. As a consequence, V'_{HI} , and therefore ϵ in Eq. (10) and r in Eq. (12b) – see Fig. 2-(b) –, decrease sharply (enhancing N_{HI^*}), whereas $|V''_{\text{HI}}|$ (or $|\eta|$) increases adequately, thereby lowering n_s within the range of Eq. (13a). In particular, for constant κ , the lower the value for n_s we wish to attain, the closer we must set σ_* to σ_{\max} . To quantify the amount of these tunings, we define the quantities

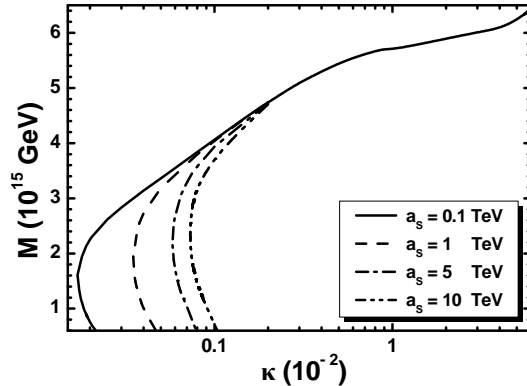
$$\Delta_{c^*} = \frac{\sigma_* - \sigma_c}{\sigma_c} \quad \text{and} \quad \Delta_{\max^*} = \frac{\sigma_{\max} - \sigma_*}{\sigma_{\max}} \quad (16)$$

and list their resulting values in Table I. From there, we conclude that the required tuning is at a few percent level, since $\Delta_{c^*}, \Delta_{\max^*} \leq 10\%$. Values of a_S well below 1 TeV are less desirable from this point of view. For comparison, we mention that for $\kappa \geq 0.002$, we get $\Delta_{c^*} \geq 30\%$, i.e., Δ_{c^*} increases with κ whereas the maximum disappears. From Table I, we note that κ and M decrease with Δ_{c^*} and Δ_{\max^*} , too.

In Fig. 2-(a) and Fig. 2-(b) respectively we display the predictions of our model for $|\alpha_s| \equiv |dn_s/d \ln k|$ and r . Corresponding to the n_s values within Eq. (13a), $|\alpha_s|$ turns out to be of order 10^{-4} . On the contrast, r is extremely tiny, of order $10^{-14} - 10^{-12}$, and therefore far outside the reach of PLANCK and other contemporary experiments. For the preferred n_s values, we observe that r and $|\alpha_s|$ increase with a_S whereas for constant a_S , α_s , and r increase with n_s . For the a_S values used in Fig. 2 and with $n_s = 0.96$, our predictions are summarized in Table I.

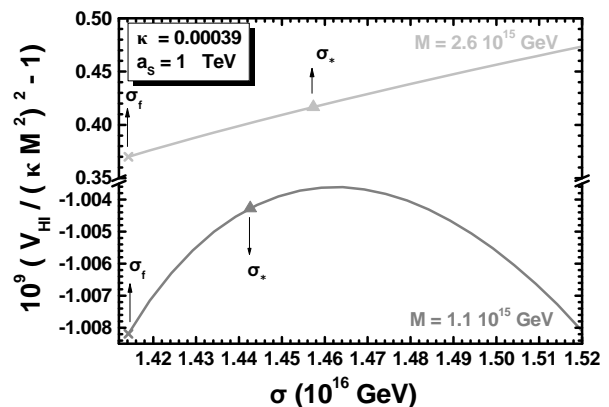
The dependence of M on κ within our model is shown in Fig. 3. We remark that M mostly decreases with κ . For low enough κ values, there is region where we get two M values consistent with Eqs. (9) and (11). Comparing Fig. 3 with Fig. 1-(b), we can easily conclude that the latter solution is consistent with Eq. (13a). The M values displayed in this figure are fully compatible with the upper bound arising from Eq. (14). Although these M values lie somewhat below M_{GUT} , the unification of gauge coupling constants within MSSM remains intact since the gauge boson associated with the spontaneous $U(1)_{B-L}$ breaking is neutral under G_{MSSM} , and so it does not contribute to the relevant *renormalization group* (RG) running.

In order to highlight the differences of the various possible solutions obtained at low κ values, we present in Fig. 4 the variation of V_{HI} as a function of σ for the same κ and a_S and two different M values compatible with Eqs. (9) and (11). Namely, we take $a_S = 1$ TeV, $\kappa = 3.9 \cdot 10^{-4}$ and $M =$


FIG. 3: M versus κ for various a_S values.

$1.1 \cdot 10^{15}$ GeV [$M = 2.6 \cdot 10^{15}$ GeV] yielding $n_s = 0.96$ [$n_s = 0.994$] with $\Delta_{c^*} = 2\%$ [$\Delta_{c^*} = 3\%$] – gray [light gray] line. The corresponding σ_* and σ_f values are also shown. As we anticipated above, in the first case, V_{HI} develops a maximum at $\sigma_{\max} \simeq 1.46M$ decreasing thereby n_s at an acceptable level – we get $\Delta_{\max^*} = 1.2\%$ as shown in Table I. Needless to say that, in both cases, V_{HI} turns out to be bounded from below for large σ values and, therefore, no complications arise in the realization of the inflationary dynamics.

As inferred from Fig. 1, for any $\kappa \lesssim 10^{-4}$ we can conveniently adjust a_S , so that Eq. (13a) is fulfilled. Working in this direction, we delineate the (lightly gray) region in the $\kappa - a_S$ [$M - a_S$] plane allowed by all the imposed constraints – see Fig. 5-(a) [Fig. 5-(b)]. We also display by solid lines the allowed contours for $n_s = 0.96$. We do not consider a_S values lower than 0.1 TeV, since they would be less natural from the point of view of both SUSY breaking and the Δ_{c^*} 's and Δ_{\max^*} 's encountered – see Table I. The boundaries of the allowed areas in Fig. 5 are determined by the dashed [dot-dashed] lines corresponding to the lower [upper] bound on n_s in Eq. (13a). In these regions we ob-


FIG. 4: The variation of V_{HI} as a function of σ for $a_S = 1$ TeV, $\kappa = 3.9 \cdot 10^{-4}$ and $M = 1.1 \cdot 10^{15}$ GeV ($n_s = 0.96$, gray line) or $M = 2.6 \cdot 10^{15}$ GeV ($n_s = 0.994$, light gray line).

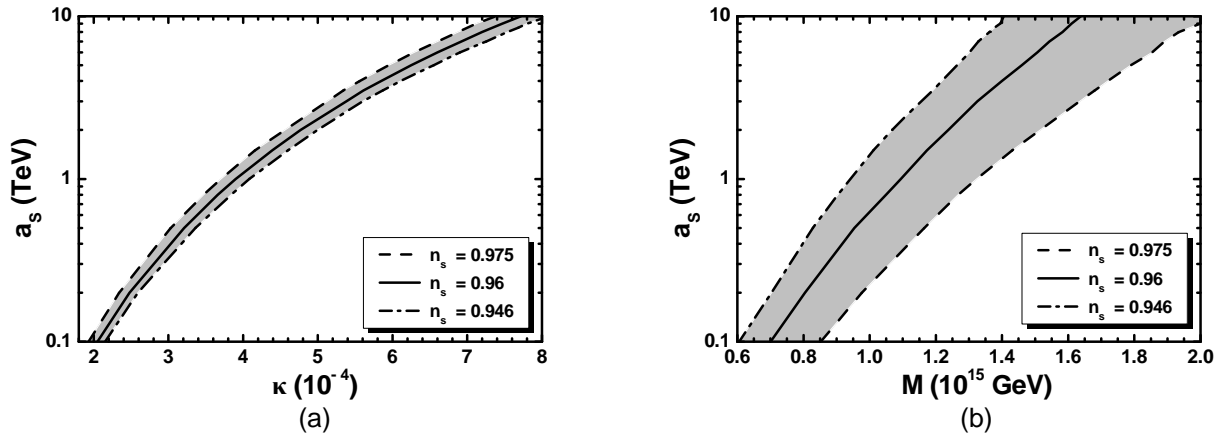


FIG. 5: Allowed (shaded) regions as determined by Eqs. (9), (11), (13a) and (14) in (a) $\kappa - a_S$ plane and (b) $M - a_S$ plane. The n_s values for the various lines are also shown.

tain $m_{\nu_{cs}} = (0.98 - 12.4) \cdot 10^{-7} m_{\text{P}}^2$ which are compatible with Eq. (14). On the other hand, these regions are not consistent with the most stringent (although controversial [32]) constraint $\mu_{cs} \lesssim 10^{-7} m_{\text{P}}^2$ [33] imposed by the limit on the stochastic gravitational wave background from the European Pulsar Timing Array. These latter results depend on assumptions regarding string loop formation and the gravitational waves emission. The bounds on M from μ_{cs} , are totally avoided if we implement FHI within G_{LR} [4] or flipped $SU(5)$ [5], with $N = 2$ or $N = 10$ respectively in Eq. (6a), which do not lead to the production of any cosmic defect – for a more complete discussion involving flipped $SU(5)$ and the corresponding M values, see second paper in [6].

Summarizing our findings from Fig. 5, for n_s considered by Eq. (13a) and $0.1 \lesssim a_S/\text{TeV} \lesssim 10$, we obtain:

$$1.9 \lesssim \kappa/10^{-4} \lesssim 8.1, \quad 0.6 \lesssim M/10^{15} \text{ GeV} \lesssim 2, \quad (17a)$$

$$1.1 \lesssim |\alpha_s|/10^{-3} \lesssim 2.8, \quad 0.05 \lesssim r/10^{-13} \lesssim 76. \quad (17b)$$

The M values are consistent with Eq. (14) according to which $M \lesssim (5 - 5.45) \cdot 10^{15} \text{ GeV}$. The maximal values for $|\alpha_s|$ and r are respectively encountered in the upper left and right corners of the allowed region in Fig. 5-(b). In the lower left [right] corner of that area, we obtain the lowest possible r [$|\alpha_s|$]. Also, Δ_{c^*} ranges between 0.6% and 7.3% whereas Δ_{max^*} varies between 0.001% and 7.9%.

III. NON-THERMAL LEPTOGENESIS

A. INFLATON DECAY. As FHI ends, σ crosses σ_c , thereby destabilizing the $\Phi - \bar{\Phi}$ system which leads to a stage of tachyonic preheating as described in Ref. [28]. Soon afterwards, the inflaton system (IS) settles into a phase of damped oscillations about the SUSY vacuum, eventually decaying and reheating the universe. Note that the IS consists of the two complex scalar fields S and $(\delta\bar{\Phi} + \delta\Phi)/\sqrt{2}$, where $\delta\bar{\Phi} = \bar{\Phi} - M$ and $\delta\Phi = \Phi - M$. To ensure the decay of the IS and implement the see-saw mechanism for the generation of the light neutrino

masses, we allow for the following superpotential terms:

$$W_{\text{RHN}} = \lambda_i \bar{\Phi} \nu_i^c \nu_i^c + h_{Nij} \nu_i^c L_j H_u, \quad (18)$$

where $\bar{\Phi} [\nu_i^c]$ have $B - L$ charge of $-2[1]$ and R charge 0 [$\alpha/2$]. L_i denotes the i -th generation $SU(2)_L$ doublet left-handed lepton superfields, and H_u is the $SU(2)_L$ doublet Higgs superfield which couples to the up quark superfields.

At the SUSY vacuum, Eq. (3), Φ and $\bar{\Phi}$ acquire their v.e.v.s, thereby providing masses to the IS and ν_i^c 's,

$$(a) \quad m_I = \sqrt{2}\kappa M \quad \text{and} \quad (b) \quad M_{i\nu^c} = 2\lambda_i M. \quad (19)$$

The predominant decay channels of S and $(\delta\bar{\Phi} + \delta\Phi)/\sqrt{2}$ are to (kinematically allowed) bosonic and fermionic ν_i^c 's respectively via tree-level couplings derived from Eqs. (1) and (18) – see e.g. Ref. [23] – with almost the same decay width [27]

$$\Gamma_{I \rightarrow \nu_i^c} = \frac{1}{64\pi} \lambda_i^2 m_I \sqrt{1 - 4M_{i\nu^c}^2/m_I^2}. \quad (20)$$

We assume here that the μ problem of MSSM is resolved as suggested in Ref. [5, 35], rather than by invoking the mechanism of Ref. [4] which would open new and efficient decay channels for S . The SUGRA-induced [36] decay channels are negligible in our set-up, with the M and m_I values in Eq. (17a). The resulting reheat temperature is given by [34]

$$T_{\text{rh}} \approx (72/5\pi^2 g_*)^{1/4} \sqrt{\sum_i \Gamma_{I \rightarrow \nu_i^c} m_{\text{P}}}, \quad (21)$$

where $g_* = 228.75$ counts the MSSM effective number of relativistic degrees of freedom at temperature T_{rh} .

For $T_{\text{rh}} < M_{i\nu^c}$, the out-of-equilibrium decay of ν_i^c generates a lepton-number asymmetry (per ν_i^c decay), ε_i . The resulting lepton-number asymmetry is partially converted through sphaleron effects into a yield of the observed BAU:

$$Y_B = -0.35 \cdot 2 \cdot \frac{5 T_{\text{rh}}}{4 m_I} \sum_i \text{Br}_i \varepsilon_i, \quad \text{with} \quad \text{Br}_i = \frac{\Gamma_{I \rightarrow \nu_i^c}}{\sum_i \Gamma_{I \rightarrow \nu_i^c}} \quad (22)$$

being the branching ratio of IS to ν_i^c . The quantity ε_i can be expressed in terms of the Dirac masses of ν_i , m_{iD} , arising from the second term of Eq. (18).

The required T_{rh} in Eq. (22) must be compatible with constraints on the gravitino (\tilde{G}) abundance, $Y_{3/2}$, at the onset of nucleosynthesis (BBN), which is estimated to be [18]:

$$Y_{3/2} \simeq 1.9 \cdot 10^{-22} T_{\text{rh}}/\text{GeV}, \quad (23)$$

where we take into account only thermal production of \tilde{G} , and assume that \tilde{G} is much heavier than the MSSM gauginos – the case of \tilde{G} CDM was recently analyzed in Ref. [28].

B. POST-INFLATIONARY REQUIREMENTS. The success of our post-inflationary scenario can be judged, if, in addition to the constraints of Sec. II, it is consistent with the following requirements:

- The bounds on $M_{i\nu^c}$:

$$M_{i\nu^c} \lesssim 7.1M, \quad M_{1\nu^c} \gtrsim 10T_{\text{rh}} \quad \text{and} \quad m_I \geq 2M_{i\nu^c}, \quad (24)$$

for some ν_i^c 's. The first bound comes from the needed perturbativity of λ_i 's in Eq. (18), i.e. $\lambda_i \leq \sqrt{4\pi}$. The second inequality is applied to avoid any erasure of the produced Y_L due to ν_1^c mediated inverse decays and $\Delta L = 1$ scatterings [40]. Finally, the last bound above ensures a kinematically allowed decay of the IS for some ν_i^c 's.

- Constraints from Neutrino Physics. We take as inputs the best-fit values [19] – see also Ref. [20] – on the neutrino mass-squared differences, $\Delta m_{21}^2 = 7.62 \cdot 10^{-3} \text{ eV}^2$ and $\Delta m_{31}^2 = (2.55 [-2.43]) \cdot 10^{-3} \text{ eV}^2$, on the mixing angles, $\sin^2 \theta_{12} = 0.32$, $\sin^2 \theta_{13} = 0.0246 [0.025]$, and $\sin^2 \theta_{23} = 0.613 [0.6]$ and the CP-violating Dirac phase $\delta = 0.8\pi [-0.03\pi]$ for *normal [inverted] ordered (NO [IO]) neutrino masses*, $m_{i\nu}$'s. The sum of $m_{i\nu}$'s is bounded from above by the data [13, 15], $\sum_i m_{i\nu} \leq 0.28 \text{ eV}$ at 95% c.l.

- The observational results on Y_B [13, 15]

$$Y_B \simeq (8.55 \pm 0.217) \cdot 10^{-11} \quad \text{at 95\% c.l.} \quad (25)$$

- The bounds on $Y_{3/2}$ imposed [18] by successful BBN:

$$Y_{3/2} \lesssim \begin{cases} 10^{-14} \\ 4.3 \cdot 10^{-14} \\ 10^{-13} \end{cases} \quad \text{for } m_{3/2} \simeq \begin{cases} 0.69 \text{ TeV} \\ 8 \text{ TeV} \\ 10.6 \text{ TeV} \end{cases} \quad (26)$$

Here we consider the conservative case where \tilde{G} decays with a tiny hadronic branching ratio.

C. RESULTS. The inflationary requirements of Sec. II restrict κ and M in the very narrow range presented in Eq. (17a). As a consequence, the mass m_I of IS given by Eq. (19), is confined to the range $(2 - 17.8) \cdot 10^{11} \text{ GeV}$, and its variation is not expected to decisively influence our results on Y_B . For this reason, throughout our analysis here we use the central value $m_I \simeq 6 \cdot 10^{11} \text{ GeV}$, corresponding to the second row of Table I.

On the other hand, T_{rh} (and Y_B) also depend on the masses $M_{i\nu^c}$ of ν_i^c into which the IS decays. Following the bottom-up approach – see Sec. IVB of Ref. [38] –, we find the $M_{i\nu^c}$'s

TABLE II: Parameters yielding the correct BAU for $\kappa = 0.00039$, $a_S = 1 \text{ TeV}$ and various neutrino mass schemes.

Parameters	Cases						
	A	B	C	D	E	F	G
	Normal Hierarchy		Degenerate Masses			Inverted Hierarchy	
Low Scale Parameters							
$m_{1\nu}/0.1 \text{ eV}$	0.01	0.1	0.5	0.7	0.7	0.5	0.49
$m_{2\nu}/0.1 \text{ eV}$	0.09	0.13	0.51	1.0	0.705	0.51	0.5
$m_{3\nu}/0.1 \text{ eV}$	0.5	0.51	0.71	1.12	0.5	0.1	0.05
$\sum_i m_{i\nu}/0.1 \text{ eV}$	0.6	0.74	1.7	2.3	1.9	1.1	1
φ_1	0	$\pi/3$	0	$\pi/2$	0	$-\pi/6$	0
φ_2	0	0	$\pi/3$	0	$-\pi/2$	0	$-\pi/3$
Leptogenesis-Scale Parameters							
$m_{1D}/0.1 \text{ GeV}$	1.67	4.1	3.7	7	7	5	60
m_{2D}/GeV	4	0.5	1.1	1.55	1.03	0.93	4
m_{3D}/GeV	120	120	5	2	2	4	1.32
$M_{1\nu^c}/10^9 \text{ GeV}$	2.5	2.4	3.3	6.5	4.6	1	48
$M_{2\nu^c}/10^{10} \text{ GeV}$	47	1.6	1.7	2.7	1.6	2.8	59
$M_{3\nu^c}/10^{12} \text{ GeV}$	3720	580	0.34	0.035	0.046	0.7	10
Decay channels of the Inflaton System, I							
I \rightarrow	ν_1^c	$\nu_{1,2}^c$	$\nu_{1,2}^c$	$\nu_{1,2,3}^c$	$\nu_{1,2,3}^c$	$\nu_{1,2}^c$	ν_1^c
Resulting B -Yield							
$10^{11} Y_B^0$	8.9	8.25	8	6	6.9	8.3	11.1
$10^{11} Y_B$	8.5	8.6	8.6	8.6	8.5	8.5	8.6
Resulting T_{rh} and \tilde{G} -Yield							
$T_{\text{rh}}/10^8 \text{ GeV}$	0.7	2	1.9	4.1	5.5	3	5
$10^{14} Y_{3/2}$	1.3	3.8	3.6	9.5	10	6	10

by using as inputs the m_{iD} 's, a reference mass of the ν_i 's – $m_{1\nu}$ for NO $m_{i\nu}$'s, or $m_{3\nu}$ for IO $m_{i\nu}$'s –, the two Majorana phases φ_1 and φ_2 of the MNS matrix, and the best-fit values mentioned above for the low energy parameters of neutrino physics. In our numerical code, we also estimate, following Ref. [39], the RG evolved values of the latter parameters at the scale of nTL, $\Lambda_L = m_I$, by considering the MSSM with $\tan \beta \simeq 50$ as an effective theory between Λ_L and the SUSY-breaking scale, $M_{\text{SUSY}} = 1.5 \text{ TeV}$. We evaluate the $M_{i\nu^c}$'s at Λ_L , and we neglect any possible running of the m_{iD} 's and $M_{i\nu^c}$'s. Therefore, we present their values at Λ_L .

Our results are displayed in Table II taking some representative values of the parameters which yield the correct Y_B , as dictated by Eq. (25). We consider NO (cases A and B), degenerate (cases C, D and E) and IO (cases F and G) $m_{i\nu}$'s. In all cases the current limit (see point 2 above) on the sum of $m_{i\nu}$'s is safely met – the case D approaches it. The gauge group adopted here, G_{B-L} , does not predict any relation between the Yukawa couplings constants h_N entering the second term of Eq. (18) and the other Yukawa couplings in the MSSM. As

a consequence, the m_{iD} 's are free parameters. However, for the sake of comparison, for case A, we take $m_{3D} = m_t(\Lambda_L)$, and in case B, we also set $m_{2D} = m_c(\Lambda_L)$, where m_t and m_c denote the masses of the top and charm quark respectively. We observe that in all cases $m_{1D} \gtrsim 0.1$ GeV. This is done, in order to fulfill the second inequality in Eq. (24), given that m_{1D} heavily influences $M_{1\nu c}$. Note that such an adjustment requires theoretical motivation, if the gauge group is G_{LR} or flipped $SU(5)$ – cf. Ref. [40].

From Table II we observe that with NO or IO $m_{i\nu}$'s, the resulting $M_{i\nu c}$'s are also hierarchical. With degenerate $m_{i\nu}$'s, the resulting $M_{i\nu c}$'s are closer to one another. Therefore, in the latter case more IS-decay channels are available, whereas for cases A and G only a single decay channel is open. In all other cases, the dominant contributions to Y_B arise from ε_2 . In Table II we also display, for comparison, the B -yield with (Y_B) or without (Y_B^0) taking into account the RG effects. We observe that the two results are mostly close to each other with some discrepancies appearing for degenerate and IO $m_{i\nu}$'s. Shown also are values for T_{rh} , the majority of which are close to $5 \cdot 10^8$ GeV, and the corresponding $Y_{3/2}$'s, which are consistent with Eq. (26) mostly for $m_{3/2} \gtrsim 8$ TeV. These large values can be comfortably tolerated with the a_S 's appearing in Fig. 5 for $A \sim 1$ – see the definition of a_S below Eq. (8). From the perspective of \tilde{G} constraint, case A turns out to be the most promising.

IV. CONCLUSIONS

Inspired by the recently released WMAP and PLANCK results for the inflationary observables, we have reviewed

and updated the predictions arising from a minimal model of SUSY (F-term) hybrid inflation, also referred to as FHI. In this set-up [1], FHI is based on a unique renormalizable superpotential, employs a canonical Kähler potential, and is associated with a superheavy $B - L$ phase transition. As shown in Ref. [6], and verified by us here, to achieve n_s values lower than 0.98, one should include in the inflationary potential the soft SUSY breaking tadpole term, with the SUSY breaking mass parameter values in the range (0.1 – 10) TeV. Fixing n_s to its central value, the dimensionless coupling constant, the $B - L$ symmetry breaking scale, and the inflationary parameters α_s and r are respectively given by $\kappa = (2 - 7.7) \cdot 10^{-4}$, $M = (0.7 - 1.6) \cdot 10^{15}$ GeV, $|\alpha_s| \simeq (1.5 - 2.5) \cdot 10^{-4}$ and $r \simeq (0.1 - 37) \cdot 10^{-13}$. The $B - L$ cosmic strings, formed at the end of FHI, have tension ranging from 1.3 to $8.3 \cdot 10^{-7} m_{\text{P}}^2$ and may be accessible to future observations. We have also briefly discussed the reheat temperature, gravitino constraints and non-thermal leptogenesis taking into account updated values for the neutrino oscillation parameters.

ACKNOWLEDGMENTS

Q.S. acknowledges support by the DOE grant No. DE-FG02-12ER41808. We would like to thank W. Buchmüller, M. Hindmarsh, A. Mazumdar and K. Schmitz for useful discussions.

REFERENCES

- [1] G.R. Dvali, Q. Shafi and R.K. Schaefer, *Phys. Rev. Lett.* **73**, 1886 (1994) [hep-ph/9406319].
- [2] E.J. Copeland *et al.*, *Phys. Rev. D* **49**, 6410 (1994) [astro-ph/9401011].
- [3] V.N. Şenoğuz and Q. Shafi, hep-ph/0512170.
- [4] G.R. Dvali, G. Lazarides and Q. Shafi, *Phys. Lett. B* **424**, 259 (1998) [hep-ph/9710314].
- [5] B. Kyae and Q. Shafi, *Phys. Lett. B* **635**, 247 (2006) [hep-ph/0510105].
- [6] M.U. Rehman, Q. Shafi and J.R. Wickman, *Phys. Lett. B* **683**, 191 (2010) [arXiv:0908.3896]; M. U. Rehman, Q. Shafi and J. R. Wickman, *Phys. Lett. B* **688**, 75 (2010) [arXiv:0912.4737]; M. Civeletti, M. U. Rehman, E. Sabo, Q. Shafi and J. Wickman, arXiv:1303.3602.
- [7] A.D. Linde and A. Riotto *Phys. Rev. D* **56**, 1841 (1997) [hep-ph/9703209]; V.N. Şenoğuz and Q. Shafi, *Phys. Lett. B* **567**, 79 (2003) [hep-ph/0305089].
- [8] V.N. Şenoğuz and Q. Shafi, *Phys. Rev. D* **71**, 043514 (2005) [hep-ph/0412102].
- [9] M. Bastero-Gil, S.F. King, and Q. Shafi, *Phys. Lett. B* **651**, 345 (2007) [hep-ph/0604198]; B. Garbrecht *et al.*, *J. High Energy Phys.* **12**, 038 (2006) [hep-ph/0605264]; M.U. Rehman, V.N. Şenoğuz, and Q. Shafi, *Phys. Rev. D* **75**, 043522 (2007) [hep-ph/0612023]; C. Pallis, *J. Cosmol. Astropart. Phys.* **04**, 024 (2009) [arXiv:0902.0334].
- [10] M.U. Rehman, Q. Shafi and J.R. Wickman, *Phys. Rev. D* **83**, 067304 (2011) [arXiv:1012.0309].
- [11] R. Armillius and C. Pallis, “Recent Advances in Cosmology”, edited by A. Travena and B. Soren (Nova Science Publishers Inc., New York, 2013) [arXiv:1211.4011].
- [12] G. Lazarides and C. Pallis, *Phys. Lett. B* **651**, 216 (2007) [hep-ph/0702260].
- [13] G. Hinshaw *et al.* [WMAP Collaboration], arXiv:1212.5226.
- [14] P.A.R. Ade *et al.* [Planck Collaboration], arXiv:1303.5082.
- [15] P.A.R. Ade *et al.* [Planck Collaboration], arXiv:1303.5076.
- [16] G. Lazarides and Q. Shafi, *Phys. Lett. B* **258**, 305 (1991); K. Kumekawa, T. Moroi and T. Yanagida, *Prog. Theor. Phys.* **92**, 437 (1994) [hep-ph/9405337]; G. Lazarides, R.K. Schaefer and Q. Shafi, *Phys. Rev. D* **56**, 1324 (1997) [hep-ph/9608256]; V.N. Şenoğuz and Q. Shafi, *Phys. Rev. D* **71**, 043514 (2005) [hep-ph/0412102].
- [17] M.Yu. Khlopov and A.D. Linde, *Phys. Lett. B* **138**, 265 (1984); J. Ellis, J.E. Kim, and D.V. Nanopoulos, *ibid.* **145**, 181 (1984).
- [18] M.Kawasaki, K.Kohri and T.Moroi, *Phys. Lett. B* **625**, 7 (2005) [astro-ph/0402490]; M. Kawasaki, K. Kohri and T. Moroi, *Phys. Rev. D* **71**, 083502 (2005) [astro-ph/0408426];

- R.H. Cyburt *et al.*, *Phys. Rev. D* **67**, 103521 (2003) [astro-ph/0211258]; J.R. Ellis, K.A. Olive and E. Vangioni, *Phys. Lett. B* **619**, 30 (2005) [astro-ph/0503023].
- [19] D.V. Forero, M. Tortola and J.W.F. Valle, *Phys. Rev. D* **86**, 073012 (2012) [arXiv:1205.4018].
- [20] G.L. Fogli *et al.*, *Phys. Rev. D* **86**, 013012 (2012) [arXiv:1205.5254].
- [21] P.A.R. Ade *et al.* [Planck Collaboration], arXiv:1303.5085.
- [22] M. Hindmarsh, *Prog. Theor. Phys. Suppl.* **190**, 197 (2011) [arXiv:1106.0391]; D.M. Regan, arXiv:1112.5899 and references therein.
- [23] G. Lazarides, *Lect. Notes Phys.* **592**, 351 (2002) [hep-ph/0111328]; G. Lazarides, *J. Phys. Conf. Ser.* **53**, 528 (2006) [hep-ph/0607032].
- [24] D.H. Lyth and A. Riotto, *Phys. Rept.* **314**, 1 (1999) [hep-ph/9807278]; A. Mazumdar and J. Rocher, *Phys. Rept.* **497**, 85 (2011) [arXiv:1001.0993].
- [25] S. Clesse, *Phys. Rev. D* **83**, 063518 (2011) [arXiv:1006.4522]; H. Kodama, K. Kohri, and K. Nakayama, *Prog. Theor. Phys.* **126**, 331 (2011) [arXiv:1102.5612]; S. Clesse and B. Garbrecht, *Phys. Rev. D* **86**, 023525 (2012) [arXiv:1204.3540].
- [26] J. Rocher and M. Sakellariadou, *J. Cosmol. Astropart. Phys.* **03**, 004 (2005) [hep-ph/0406120]; R. Jeannerot and M. Postma, *J. High Energy Phys.* **05**, 071 (2005) [hep-ph/0503146].
- [27] K. Nakayama *et al.*, *J. Cosmol. Astropart. Phys.* **12**, 010 (2010) [arXiv:1007.5152].
- [28] W. Buchmüller, V. Domcke and K. Schmitz, *Nucl. Phys.* **B862**, 587 (2012) [arXiv:1202.6679].
- [29] A. Basboll, M. Hindmarsh and D.R.T. Jones, *J. High Energy Phys.* **06**, 115 (2011) [arXiv:1101.5622].
- [30] R. Battye, B. Garbrecht and A. Moss, *Phys. Rev. D* **81**, 123512 (2010) [arXiv:1001.0769]; J. Urrestilla, N. Bevis, M. Hindmarsh and M. Kunz, *J. Cosmol. Astropart. Phys.* **12**, 021 (2011) [arXiv:1108.2730].
- [31] L. Boubekeur and D. Lyth, *J. Cosmol. Astropart. Phys.* **07**, 010 (2005) [hep-ph/0502047]; K. Kohri, C.M. Lin and D.H. Lyth, *J. Cosmol. Astropart. Phys.* **12**, 004 (2007) [arXiv:0707.3826]; C.M. Lin and K. Cheung, *J. Cosmol. Astropart. Phys.* **03**, 012 (2009) [arXiv:0812.2731].
- [32] S.A. Sanidas, R.A. Battye and B. W. Stappers, *Phys. Rev. D* **85**, 122003 (2012) [arXiv:1201.2419].
- [33] R. van Haasteren *et al.*, arXiv:1103.0576.
- [34] C. Pallis, *Nucl. Phys.* **B751**, 129 (2006) [hep-ph/0510234].
- [35] G. Lazarides and Q. Shafi, *Phys. Rev. D* **58**, 071702 (1998) [hep-ph/9803397].
- [36] M. Endo, F. Takahashi and T.T. Yanagida, *Phys. Rev. D* **76**, 083509 (2007) [arXiv:0706.0986].
- [37] M. Bolz, A. Brandenburg and W. Buchmüller, *Nucl. Phys.* **B606**, 518 (2001); M. Bolz, A. Brandenburg and W. Buchmüller, *Nucl. Phys.* **B790**, 336 (2008) (E) [hep-ph/0012052]; J. Pradler and F.D. Steffen, *Phys. Rev. D* **75**, 023509 (2007) [hep-ph/0608344].
- [38] C. Pallis and Q. Shafi, *Phys. Rev. D* **86**, 023523 (2012) [arXiv:1204.0252].
- [39] S. Antusch, J. Kersten, M. Lindner and M. Ratz, *Nucl. Phys.* **B674**, 401 (2003) [hep-ph/0305273].
- [40] V.N. Şenoğuz, *Phys. Rev. D* **76**, 013005 (2007) [arXiv:0704.3048].